Supplemental Information

System & Methods

Initial Dimer Structures. For the calculations presented in this work, two initial dimer structures were selected. These two structures are termed the "extended" and "hairpin" structures throughout the paper. Both structures are derived from possible configurations of 2 Aβ units within a full fibril structure. All Aβ structures used in this work are the 42 residue peptides. The structure of Aβ peptides within a fibril is still controversial as there appears to be a significant amount of heterogeneity in fibril structure[1-3]. The extended dimer represents a separate dimer unit that has been observed within fibrils[1] where two C-terminal units of adjacent Aβ peptides are shared in an antiparallel structure with non-interacting N-termini. As a crystal structure for the fibril did not exist at the time of these simulations, an idealized structure was manually created from a 42 residue monomer unit within the 2BEG structure. To create the extended C-terminal region, the monomer was placed in a vacuum and a constraint was placed between residue 17 and residue 42 of the peptide. GROMACS 4.0[4-6] was used to increase the length between these residues to 7.0nm along the x-axis. A second monomer was created by translating and rotating the first monomer and the two monomers were placed in the appropriate position to create an idealized, antiparallel extended dimer, as shown in Figure 1a. The hairpin dimer represents what is believed to be the more consensus structure for a dimer unit within a fibril. The hairpin unit is taken as two monomers from the Protein Database (PDB) code 2BEG fibril structure[3] as edited to include the full N-terminal residues as described in our previous work and pictured in Figure 1b of that work[7]. In order to create the ideal hairpin dimer structure, we added the appropriate N-terminal residues to a monomer from the 2BEG structure, then spaced two 42 residue Aβ monomers to exactly reproduce a 2 unit structure from within the 2BEG file (Figure 1b). For all structures used in this work, the N-terminus was represented by NH_3^+ and the C-terminus was represented by COO^-. Further, a united atom GROMOS96 forcefield[4-6] was used in all calculations to represent the dimer.

As mentioned in our previous works[7,8], anionic lipids are able to decrease the local pH near the bilayer surface due to attraction of H^+ ions from solution to the headgroups at the bilayer surface[9,10]. For Aβ it has been shown that binding of the peptide to a purely anionic palmitoyloleoylphosphatidylglycerol membrane is sufficient to protonate the three histidine residues on Aβ[9]. At a physiological pH, Aβ has a net charge of -3. However, upon binding to anionic lipids, the protonation of these three key histidine residues changes the net charge to neutral. Thus, it is important to study Aβ at both the charged and neutral states. We repeated the above procedure for dimer creation for both the charged and neutral states of Aβ. The charge on the histidines was changed using utilities within GROMACS[4-6].

Once the idealized dimers were created, it was clear that they were unlikely to be stable in their ideal structures and required significant equilibration. Both dimers were solvated in a large box of SPC/E water molecules[11], a steepest descent energy minimization was used to remove clashes in the system, and a short 8ns MD simulation was performed under constant pressure (NPT) conditions to equilibrate the structure. For the charged system, 6 Na^+ ions were added for charge neutrality. For the neutral system, no ions were added. After the short equilibration, a full 150ns MD simulation was performed under the same conditions in order to

compare the stability of these idealized structures in solution versus on the bilayer surface during equilibration. For these simulations and all future simulations, including the umbrella sampling simulations, temperature was held constant at 323K using a Nosé-Hoover scheme[12] with a relaxation time of 0.5ps. All bonds were constrained using the P-LINCS algorithm[13]. For the full MD steps during all production runs, both during equilibration and umbrella sampling, this constraint allowed for a 3ps time step. Long-range electrostatics used the SPME algorithm[14] with periodic boundary conditions applied in all three dimensions. SPC/E water[11] was used for all simulations. For the systems described under NPT conditions, a Parrinello-Rahman pressure coupling scheme[15] was used with a barostat relaxation time of 0.5ps at a pressure of 1atm. For all umbrella sampling simulations, a constant volume (NVT) constraint was used. If the system was not specifically described as being under NPT conditions, then the system was under a constant volume (NVT) constraint. Secondary structure during the full MD simulations in solution was calculated using the DSSP algorithm[16] with GROMACS.

Thermodynamic Cycle Calculations. The goal of this work is to study Aβ dimerization on the bilayer surface. As described in more detail in the Discussion section, direct calculation of this value through umbrella sampling MD simulations would be exceptionally cumbersome and fraught with potential sources of error. Thus, we have decided to use a thermodynamic cycle to calculate this dimerization free energy indirectly. As demonstrated in Figure 2, we are able to calculate a value for $\Delta G_{Dimerization}$ through use of the relationship:

$$2*\Delta G_{Binding} + \Delta G_{Dimerization} + \Delta G_{Release} + \Delta G_{Dissociation} = 0 \quad (1)$$

As long as the final structures for the dimer dissociation process results in two equilibrated, non-interacting monomers in solution, the above relationship should hold. The values for $\Delta G_{Binding}$ were calculated for an equilibrated Aβ monomer in a previous work[7]. Further, values for $\Delta G_{Release}$ and $\Delta G_{Dissociation}$ can be calculated directly using umbrella sampling techniques[17,18]. The process of dimer release and dimer dissociation does not have as significant of sources of error as the direct calculation of $\Delta G_{Dimerization}$. Thus, the use of this thermodynamic cycle allows us to study the dimerization of Aβ using a more accurate technique considering the current restrictions of computational power available today. Of note, the dimerization free energy is being calculated for only two specific dimer structures. This choice was made so that we could directly investigate how properties of the dimer structure affect the oligomerization process. Thus, the value of $\Delta G_{Dimerization}$ calculated in this work is not a generic dimerization free energy, as would be expected in experiment, but a specific dimerization free energy for a idealized structure at a given charge state.

Dimer Equilibration on the Bilayer Surface. In order to perform the umbrella sampling simulations required for our thermodynamic cycle calculations (Figure 2), it was necessary for the dimer structures to be extensively equilibrated on the bilayer surface. For the dimer release step of the cycle, the initial structure should be a well-equilibrated, specific dimer structure on the bilayer surface. Structures for the dimers after the short 8ns equilibration in solution were used for the initial structures for equilibration on the bilayer surface. In our previous work[7,8], we used a 128-lipid bilayer system. However, because the dimer is larger, we decided to use a 200-lipid system for this study in order to prevent virtual interactions through the periodic boundaries along the bilayer surface. For a model zwitterionic system, we used a

dipalmitoylphosphatidylcholine (DPPC) bilayer and, for a model anionic system, we used a dioleylphosphatidylserine (DOPS) bilayer. DPPC was chosen as the zwitterionic system due to its preponderance both in neurons[19] and in simulation studies[20] and DOPS was chosen in part because of its importance to biology[21], but also because of a similar area per headgroup value to DPPC. As we are studying protein-lipid interactions at the bilayer surface, area per headgroup is an important physical parameter with regards to charge density. These same lipids were used for our previous investigations, so bilayer equilibration was exactly as described in a previous work[7,22]. Both lipids were described using the Berger force field parameters[22].

Starting with both the equilibrated bilayer and equilibrated dimer structures, the dimer was solvated and placed at a distance away from the bilayer surface. Only the charged dimer was used in simulations with DPPC and only the neutral dimer was used in simulations with DOPS. This pairing created 4 initial conditions: charged Aβ/DPPC for the extended and hairpin dimers and neutral Aβ/DOPS for the extended and hairpin dimers. For the charged Aβ/DPPC system, $30Na^+$ and $24Cl^-$ ions were added to approximate a 0.1M NaCl system. For the neutral Aβ/DOPS system, $224Na^+$ and $24Cl^-$ ions were added. The extra 200 Na^+ ions were necessary to counteract the charge on the DOPS lipids and were already included in the equilibration process for the DOPS bilayer. A more detailed description of exactly how a similar system was built using an Aβ monomer instead of Aβ dimer is provided in a previous work[7]. After the system was built and energy minimization was applied, a short 500ps simulation was performed under NPT conditions to allow the peptide-bilayer system to reach a transient equilibration. Because of the constraints that the bilayer surface places on building a peptide-bilayer system, the dimer was originally placed in solution at approximately 2nm above the bilayer surface. A 4ns equilibration under NVT conditions was then performed with an umbrella constraint placed between the dimer center of mass and bilayer center of mass. This equilibration forces the dimer to bind to the bilayer surface without creating any significant clashes. For the simulations on DPPC, the constraint minimum was at a center of mass separation of 2.1nm while, with DOPS, the constraint minimum was at 2.4nm. A force constant of 500 kJ/(mol*nm^2) was used. After the 4ns simulations with the constraint, the umbrella constraint was removed and another 4ns equilibration simulation was performed. Once these equilibration steps were finished, the dimer was strongly bound to the bilayer surface. However, the dimer had not been given adequate time to reach equilibration on the bilayer surface. The equilibration under NVT conditions was then extended for another 150ns to allow for an extensive dimer equilibration. The secondary structure of the dimer during equilibration was calculated using the DSSP algorithm.

Dimer Release from the Bilayer Surface. To calculate the free energy for dimer release from the bilayer surface, an umbrella sampling procedure[17,18] was utilized. Umbrella sampling allows us to directly calculate this free energy while providing full MD trajectories within each umbrella that are available in order to understand the dimer removal process in a stepwise fashion. We initially attempted to pull the equilibrated dimer from the bilayer surface using the final structure of the 150ns dimer equilibration on the bilayer surface. However, upon placing a constraint on the dimer and removing the dimer from the surface, strong protein-lipid interactions led to significant bilayer disruption. To overcome this issue, we decided to model dimer release as the negative free energy of dimer binding. Using enough umbrellas and a long enough MD simulation within each umbrella, dimer binding should be similar to dimer release with regards to the potential of mean force profiles calculated using the Weighted Histogram

Analysis Method (WHAM)[23]. As long as the initial dimer structure is the same as the equilibrated dimer on the bilayer surface, the dimer will not have enough time during the quick pulling process for any substantial internal motion to change the equilibration it shared with the bilayer. The dimer structure from the final snapshot at the end of the 150ns equilibration on the bilayer surface was used for this process. Similar to the procedure for initially creating the dimer-bilayer system, the dimer was placed at a significant distance away from the pre-equilibrated lipid bilayer and solvated with SPC/E water and either $30Na^+/24Cl^-$ (charged Aβ) or $224Na^+/24Cl^-$ (neutral Aβ) ions. After energy minimization, a short 4ns equilibration was performed under NVT conditions with an umbrella restraint between the dimer center of mass and bilayer center of mass. For the charged/DPPC systems, the constraint minimum was 7.0nm and, for the neutral/DOPS system, the constraint minimum was at 8.0nm. This constraint was necessary during the equilibration to prevent any dimer-bilayer interactions. Once the system was equilibrated, umbrella sampling could be performed.

For umbrella sampling, the reaction coordinate used for the pulling process was the dimer – bilayer center of mass separation. Thirteen windows were placed between center of mass separations of 1.8nm to 6.9nm along the reaction coordinate. This results in a 0.3nm distance between windows, which allowed for adequate sampling in our previous umbrella sampling calculations[7]. A spring constant of 500 kJ/(mol*nm^2) was placed on each center of mass separation. Starting from the same initial condition, 150ns MD simulations were performed within each window. In our previous work[7] investigating Aβ monomer binding to lipid bilayers, 80ns simulations were performed in each window. However, because of the larger size of the dimer and the use of a larger bilayer, the lengths of MD simulations performed within each window were extended to improve upon sampling. We considered the first 5ns of each umbrella sampling simulation to be equilibration with the following 145ns MD used for analysis. Within each window, analysis was performed using either GROMACS code or the DSSP algorithm within GROMACS. Once the simulations were finished, a potential of mean force curve was calculated using the WHAM methodology adapted for in-house code. The potential of mean force curves calculated for this process are given in Figure 3a. Further, block error analysis was used to calculate the error in this process and error bars are plotted on Figure 3a along with the potential of mean force curves. The error calculations result in reasonable error bars with no error being larger then 5kcal/mol. Further, a $\Delta G_{Release}$ could be calculated from the potential of mean force curve as described previously[24]. In short, the following equation was used for this calculation, where W(z) represents the potential of mean force curve:

$$\exp\left(\frac{-\Delta G_{\text{Release}}}{k_b T}\right) = \frac{1}{l_0}\int_0^{\infty}\left(\exp\left[-\beta W(z)\right]-1\right)dz \qquad (2)$$

In obtaining $\Delta G_{Release}$, l_0 was determined as the reaction coordinate value where the potential of mean force reached a value of zero once appropriate shifting of the potential of mean force curves was performed. However, in performing these calculations, we observed that the values for $\Delta G_{Release}$ were resistant to the value chosen for l_0; thus, $\Delta G_{Release}$ was fairly robust. Values for $\Delta G_{Release}$ are provided in Table I. Also, since the values that were reported in our previous work[7] for $\Delta G_{Binding}$ were the difference between the minimum and maximum values of the potential of mean force curves, we recalculated $\Delta G_{Binding}$ from these curves using equation 2. These values

are also reported in Table I. Comparing these $\Delta G_{Binding}$ values to the values reported in the previous work[7], it is clear that there is not a significant difference between the two values and all patterns presented in the previous work hold for $\Delta G_{Binding}$.

Dimer Dissociation. To calculate the final necessary step in the thermodynamic cycle, umbrella sampling simulations were performed to approximate the dimer dissociation process. For these simulations, it was necessary to separate the two monomers from a well-equilibrated dimer in solution and allow the two monomers to reach equilibration in solution without interacting. Due to the procedure used in the dimer release calculations, a well-equilibrated dimer in solution was already available. The final dimer structure from the 6.9nm center of mass separation umbrella after 150ns of MD simulation was isolated and used as the initial structure for the dimer dissociation calculations. The isolated dimer was solvated in a large box of SPC/E water with either $30Na^+/24Cl^-$ (charged Aβ) or $24Na^+/24Cl^-$ (neutral Aβ) ions. Again, this procedure was repeated for both the extended and hairpin dimers, creating 4 initial conditions for umbrella sampling. Further, the water box was quite large (12.0 nm) along the z-axis, which was the chosen axis for the reaction coordinate, to prevent the monomers from interacting through periodic boundaries. After energy minimization, a short 1ns MD simulation was performed to allow the system to come to equilibration. After equilibration, umbrella sampling was performed. For the reaction coordinate of this system, the center of mass separation along the z-axis of the box was chosen. This coordinate ensured a final system of two separated, non-interacting monomers. Twenty umbrellas were placed between center of mass separations from 0.1nm to 5.8nm, providing a separation of 0.3nm between umbrellas. A spring constant of 500 kJ/(mol*nm^2) was placed on each center of mass separation. For the neutral Aβ hairpin dimer system, an extra umbrella was added at 6.1nm to provide further data for the largest center of mass separations. Within each umbrella, 150ns of MD simulations were performed. Similar to the dimer release step, the first 5ns was considered to be equilibration and analysis was performed on the subsequent 145ns of MD using GROMACS utilities and potential of mean force curves for dimer dissociation were calculated using WHAM adapted for in house code. The potential of mean force curves are provided in Figure 3b and the $\Delta G_{Dissociation}$, calculated using equation 2, is given in Table I. The error in the potential of mean force curves for dimer dissociation was calculated in the same manner as for the dimer release step and error bars are plotted on Figure 3b. Finally, $\Delta G_{Dimerization}$ was calculated from equation 1 and provided in Table I.

Results of Dimer Equilibration Simulations

Representative plots of the DSSP secondary structure readout are given in Figure S1. As can be seen for all four plots shown, the dimer structure is not exceptionally stable and does tend to fluctuate in all cases. In comparing the extended charged dimer in solution (Figure S1a) versus on the surface of a DPPC bilayer (Figure S1b), it is clear that the dimer in solution maintains its structure to a greater extent then the dimer on the bilayer surface. It appears that the only secondary structure feature that is maintained throughout both simulations is the turn on the second monomer approximately near residue 20 (residue 62 on the plots). In solution, a much stronger beta sheet region is formed between residues 30 and 40 on both monomers. For the extended dimer structure, this represents the region of overlap between the two monomers, where the monomers can strongly interact with each other. When this dimer is in solution, the almost entirely hydrophobic section of each monomer preferentially interacts with the other monomer over being fully exposed to the solution, thus forcing the more stable secondary structure. However, when bound to the surface of DPPC, the hydrophobic C-terminus of each monomer can preferentially interact with the interfacial region of the lipid bilayer, thus providing favorable options outside of protein-protein interactions for each monomer, which decreases the stability of the dimer secondary structure. For residues 1-20 of both monomers, which are more hydrophilic and are not able to undergo interprotein interactions between monomers due to the geometry of the dimer, the residues are mostly unstructured in either environment.

Figures S1c and S1d demonstrate the secondary structure comparison for the uncharged hairpin dimer in solution versus on the surface of the DOPS bilayer. Similar to the extended dimer, the presence of the lipid bilayer alters the stability of certain elements of secondary structure. Unlike the extended dimer, all regions of the hairpin dimer are able to undergo interprotein interactions as the two monomers are stacked on one another. In comparing dimer stability in the two environments, it is clear that β-sheet structure is stabilized to some extent both in solution and on the bilayer surface. In both environments, though, the β-sheet structure does tend to dissipate over time and the amount of dimer secondary structure decreases. This is not surprising as the secondary structure of the hairpin is largely derived from the very regular arrangement of Aβ within a fibril. By removing stabilizing interactions on both sides of the dimer unit by removing it from a fibril, it would be expected that the peptide would become more disordered. Interestingly, in solution, a turn is formed between residues 25-29 in one of the monomers that quickly dissipates on the bilayer surface. It appears that the hydrophobic residues in this turn region, such as glycine or alanine, plus the positive charged lysine 28 begin to interact with aspects of the lipid bilayer that tend to unfold this turn and disrupt the dimer structure. Further, it is also of note that the ordered, stacked β-sheet structure is maintained for longer on the bilayer surface. It is possible that the bilayer acts to replace one of the missing surfaces that is lost when the dimer structure was removed from the fibril. From the plots, though, it appears that the bilayer surface is not an ideal replacement of the fibril as the β-structure is still largely lost by the end of the 150ns simulation. For all four initial conditions that were investigated, the effects described here are consistent. The comparison of these simulations demonstrates that the lipid bilayer does play an interesting role in dimer stability and that neither of these ideal dimer structures are fully stable with regards to secondary structure either in solution or on the bilayer surface. Nevertheless, for all equilibration simulations, the two monomers do stay tightly bound to each other during the extent of the equilibrations.

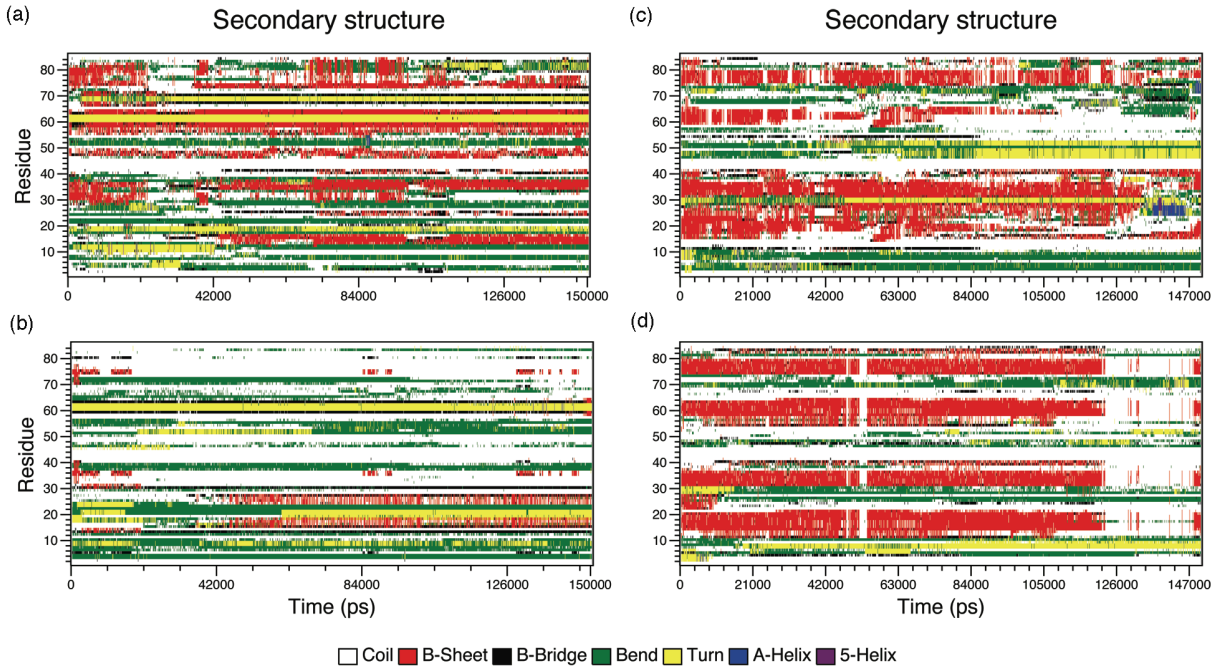

Figure S1. Secondary structure output for DSSP for 150ns equilibration simulations of Aβ42 in the following conditions: (a) Extended charged dimer in solution (b) Extended charged dimer on DPPC bilayer (c) Hairpin uncharged dimer in solution (d) Hairpin uncharged dimer on DOPS bilayer.

References for Supplemental Information

1. Sachse C, Fandrich M, Grigorieff N. Paired β-sheet structure of an Aβ(1-40) amyloid fibril revealed by electron microscopy. P Natl Acad Sci USA 2008;105(21):7462-7466.

2. Petkova AT, Ishii Y, Balbach JJ, Antzutkin ON, Leapman RD, Delaglio F, Tycko R. A structural model for Alzheimer's beta-amyloid fibrils based on experimental constraints from solid state NMR. P Natl Acad Sci USA 2002;99(26):16742-16747.

3. Luhrs T, Ritter C, Adrian M, Riek-Loher D, Bohrmann B, Doeli H, Schubert D, Riek R. 3D structure of Alzheimer's amyloid-β(1-42) fibrils. P Natl Acad Sci USA 2005;102(48):17342-17347.

4. Hess B, Kutzner C, van der Spoel D, Lindahl E. GROMACS 4: Algorithms for highly efficient, load-balanced, and scalable molecular simulation. J Chem Theory Comput 2008;4(3):435-447.

5. Van der Spoel D, Lindahl E, Hess B, Groenhof G, Mark AE, Berendsen HJC. Gromacs: Fast, Flexible, and Free. J Comput Chem 2005;26(16):1701-1718.

6. Berendsen HJC, van der Spoel D, van Drunen R. GROMACS: A message-passing parallel molecular dynamics implementation. Comput Phys Commun 1995;91(1-3):43-56.

7. Davis CH, Berkowitz ML. Interaction between amyloid-β (1-42) peptide and phospholipid bilayers: A molecular dynamics study. Biophys J 2009;96(3):785-797.

8. Davis CH, Berkowitz ML. Structure of the Amyloid-β (1-42) Monomer Absorbed To Model Phospholipid Bilayers: A Molecular Dynamics Study. J Phys Chem B 2009;113(43):14480-14486.

9. Terzi E, Holzemann G, Seelig J. Self-association of β-Amyloid peptide(1-40) in solution and binding to lipid-membranes. J Mol Biol 1995;252(5):633-642.

10. van Klompenburg W, de Kruijff B. The role of anionic lipids in protein insertion and translocation in bacterial membranes. J Membr Biol 1998;162(1):1-7.

11. Berendsen HJC, Grigera JR, Straatsma TP. The missing term in effective pair potentials. J Phys Chem-Us 1987;91(24):6269-6271.

12. Nose S. A unified formulation of the constant temperature molecular-dynamics methods. J Chem Phys 1984;81(1):511-519.

13. Hess B. P-LINCS: A parallel linear constraint solver for molecular simulation. J Chem Theory Comput 2008;4(1):116-122.

14. Essmann U, Perera L, Berkowitz ML, Darden T, Lee H, Pedersen LG. A smooth particle mesh ewald method. J Chem Phys 1995;103(19):8577-8593.

15. Parrinello M, Rahman A. Polymorphic transitions in single-crystals - a new molecular-dynamics method. J Appl Phys 1981;52(12):7182-7190.

16. Kabsch W, Sander C. Dictionary of protein secondary structure - pattern-recognition of hydrogen-bonded and geometrical features. Biopolymers 1983;22(12):2577-2637.

17. Patey GN, Valleau JP. Free-energy of spheres with dipoles - Monte-Carlo with multistage sampling. Chem Phys Lett 1973;21(2):297-300.

18. Torrie GM, Valleau JP. Non-physical sampling distributions in Monte-Carlo free-energy estimation - umbrella sampling. J Comput Phys 1977;23(2):187-199.

19. Norton WT, Abe T, Poduslo SE, DeVries GH. The lipid composition of isolated brain cells and axons. J Neurosci Res 1975;1(1):57-75.

20. Smondyrev AM, Berkowitz ML. United atom force field for phospholipid membranes: Constant pressure molecular dynamics simulation of dipalmitoylphosphatidicholine/water system. J Comput Chem 1999;20(5):531-545.

21. Elliott JI, Surprenant A, Marelli-Berg FM, Cooper JC, Cassady-Cain RL, Wooding C, Linton K, Alexander DR, Higgins CF. Membrane phosphatidylserine distribution as a non-apoptotic signalling mechanism in lymphocytes. Nat Cell Biol 2005;7(8):808-816.

22. Berger O, Edholm O, Jahnig F. Molecular dynamics simulations of a fluid bilayer of dipalmitoylphosphatidylcholine at full hydration, constant pressure, and constant temperature. Biophys J 1997;72(5):2002-2013.

23. Kumar S, Bouzida D, Swendsen RH, Kollman PA, Rosenberg JM. The weighted histogram analysis method for free-energy calculations on biomolecules .1. The method. J Comput Chem 1992;13(8):1011-1021.

24. Jamadagni SN, Godawat R, Garde S. How Surface Wettabitity Affects the Binding, Folding, and Dynamics of Hydrophobic Polymers at Interfaces. Langmuir 2009;25(22):13092-13099.